Binding of a peptide from a *Streptococcus dysgalactiae* MSCRAMM to the N-terminal F1 module pair of human fibronectin involves both modules

Ulrich Schwarz-Linek[a], Michael J. Plevin[a], Andrew R. Pickford[a], Magnus Höök[b], Iain D. Campbell[a], Jennifer R. Potts[a,*]

[a] *Department of Biochemistry, University of Oxford, South Parks Road, Oxford OX1 3QU, UK*
[b] *Center for Extracellular Matrix Biology, Institute of Bioscience and Technology, Texas A&M University System Health Center, Houston, TX 77030-3303, USA*

Received 2 March 2001; accepted 27 March 2001

First published online 10 May 2001

Edited by Thomas L. James

Abstract Host invasion by a number of pathogenic bacteria such as staphylococci and streptococci involves binding to fibronectin, a ubiquitous extracellular matrix protein. On the bacterial side, host extracellular matrix adherence is mediated by MSCRAMMs (microbial surface components recognizing adhesive matrix molecules) which, in some cases, have been identified to be important virulence factors. In this study we used nuclear magnetic resonance spectroscopy to characterize the interaction of B3, a synthetic peptide derived from an adhesin of *Streptococcus dysgalactiae*, with the N-terminal module pair ^{1}F1^{2}F1 of human fibronectin. ^{1}F1^{2}F1 chemical shift changes occurring on formation of the ^{1}F1^{2}F1/B3 complex indicate that both modules bind to the peptide and that a similar region of each module is involved. A similar surface of the ^{4}F1^{5}F1 module pair had previously been identified as the binding site for a fibronectin-binding peptide from *Staphylococcus aureus*.

Key words: Biomolecular nuclear magnetic resonance; Fibronectin; Microbial surface component recognizing adhesive matrix molecules; Protein–protein interaction

1. Introduction

Bacterial adherence to host tissue is an important step in the initiation of infection and many pathogenic bacteria bind to proteins of the human extracellular matrix (ECM). Fibronectin was the first ECM protein reported to bind specifically to *Staphylococcus aureus* [1]. The staphylococcal fibronectin-binding proteins (FnBPA and FnBPB) [2] were the first representatives of a family of bacterial cell surface adhesins called MSCRAMMs (microbial surface components recognizing adhesive matrix molecules) to be described [3]. So far at least a dozen fibronectin-binding MSCRAMMs have been discovered, particularly originating from streptococci. MSCRAMMs can be important virulence factors in bacterial infection as shown for a collagen-binding protein of *S. aureus* in experimental endocarditis [4]. Moreover, adhesion of *S. aureus* to human endothelial cells with subsequent internalization of the bacteria depends on FnBPA and FnBPB [5]. Thus the detailed study of the interactions of MSCRAMMs with their target host proteins may contribute to the development of new antimicrobial agents.

Fibronectin is a ubiquitous ECM protein. Like many proteins of the ECM it has a mosaic structure and is composed of fibronectin type 1, 2 and 3 (F1, F2 and F3) modules [6]. Fibronectin-binding MSCRAMMs from several pathogenic bacteria have a similar structural organization with the fibronectin-binding domain containing a series of three to five repeats of 40–50 residues in length. The main binding site for D1–D4 in fibronectin is the ^{4}F1^{5}F1 module pair and fibronectin residues involved in the interaction have recently been identified [7]. The FnBPB from *Streptococcus dysgalactiae* has also been shown to bind to the N-terminal region of fibronectin, but primarily to the ^{1}F1^{2}F1 module pair. In contrast to the *S. aureus* protein, rather than each of the repeats (B1–B3) containing fibronectin-binding activity, only B3 is able to bind [8].

In this study the interaction of B3 from FnBPB from *S. dysgalactiae* with ^{1}F1^{2}F1 from fibronectin is investigated using nuclear magnetic resonance (NMR) and isothermal titration calorimetry (ITC). Residues of the ^{1}F1^{2}F1 module pair that are involved in the interaction are identified.

2. Materials and methods

2.1. Sample preparation

B3 (residues 837–857 of FnBPB from *S. dysgalactiae*) was synthesized as described elsewhere [9] and purified by reverse-phase high performance liquid chromatography (HPLC). The purified peptide was checked for purity and correct molecular mass by electrospray mass spectrometry (ESMS). Both unlabeled ^{1}F1^{2}F1 (residues 17–109 of mature human fibronectin) and uniformly ^{15}N-labeled ^{1}F1^{2}F1 ([*u*-^{15}N]^{1}F1^{2}F1) were expressed in *Pichia pastoris* as described previously [10,11]. ^{1}F1^{2}F1 was purified by cation exchange chromatography and reverse-phase HPLC [10]. The purity and identity of ^{1}F1^{2}F1 (labeled and unlabeled) was confirmed by ESMS.

*Corresponding author.
E-mail: jenp@bioch.ox.ac.uk

Abbreviations: HSQC, heteronuclear single quantum coherence; ITC, isothermal titration calorimetry; MSCRAMM, microbial surface component recognizing adhesive matrix molecules; NMR, nuclear magnetic resonance; NOE, nuclear Overhauser effect; NOESY, nuclear Overhauser effect spectroscopy; TOCSY, total correlation spectroscopy

0014-5793/01/$20.00
PII: S0014-5793(01)02418-8

2.2. ITC

The experiments were carried out with a VP-ITC microcalorimeter (MicroCal Inc., Northampton, MA, USA) at 25°C. In a typical experiment the cell contained 0.12 mM $^{1}F1^{2}F1$ (1.4 ml) and the syringe contained 1.3 mM B3 (290 μl). Both solutions were in 10 mM sodium acetate buffer (pH 5.0) and were degassed at 15°C for 20 min. The titration was performed as follows: one preliminary injection of 2 μl and 44 injections of 5 μl with an injection speed of 0.5 μl/min. The stirring speed was 310 rpm and the delay time between the injections was 3 min. To take into account heats of dilution, two blank titrations were performed; one injecting B3 solution into buffer and another injecting buffer into the $^{1}F1^{2}F1$ solution. The averaged heats of dilution were subtracted from the main experiment. Data were analyzed using MicroCal Origin software (version 5.0) fitting them to a single binding site model.

2.3. NMR spectroscopy

All NMR experiments were performed on spectrometers belonging to the Oxford Centre for Molecular Sciences with ^{1}H operating frequencies of 500, 600 and 750 MHz. The spectrometers are all equipped with Oxford Instruments superconducting magnets, OMEGA software and digital control equipment (Bruker Instruments), home-built triple-resonance pulsed-field-gradient probe heads [12] and home-built linear amplifiers for ^{1}H, ^{15}N and ^{13}C nuclei. Spectra were recorded at 10, 25, or 37°C. Nuclear Overhauser effect spectroscopy (NOESY) and total correlation spectroscopy (TOCSY) spectra were acquired with 100 ms and 42 ms mixing time, respectively, unless stated otherwise. A gradient-echo technique [13] was used for suppressing the water resonance without the need for presaturation. Where required, ^{15}N decoupling during acquisition was carried out using a WALTZ16 decoupling sequence [14].

2.4. Assignment of $^{1}F1^{2}F1$

^{1}H and ^{15}N chemical shift assignments for $^{1}F1^{2}F1$ at pH 5.0 were obtained using assignments at pH 4.0 [10] and from ^{15}N-^{1}H heteronuclear single quantum coherence (HSQC) spectra of ^{15}N $^{1}F1^{2}F1$ acquired at pH 4.5 and 5.0. These assignments were confirmed using 3D ^{15}N-edited NOESY-HSQC and TOCSY-HSQC [15–17] spectra.

2.5. Assignment of $^{1}F1^{2}F1$ complexed with B3

Samples containing 1 mM B3 and 0.5 mM [u-^{15}N]$^{1}F1^{2}F1$ were prepared in either 95%/5% H_2O/D_2O or D_2O and the pH adjusted to 5.0 (uncorrected) with 1 M NaOH or HCl and NaOD and DCl, respectively. 2D ^{15}N-^{1}H HSQC [18], 2D ^{1}H-^{1}H NOESY [19–21], 2D ^{1}H-^{1}H TOCSY [22,23], 3D ^{15}N-edited NOESY-HSQC and TOCSY-HSQC [15–17] spectra were recorded.

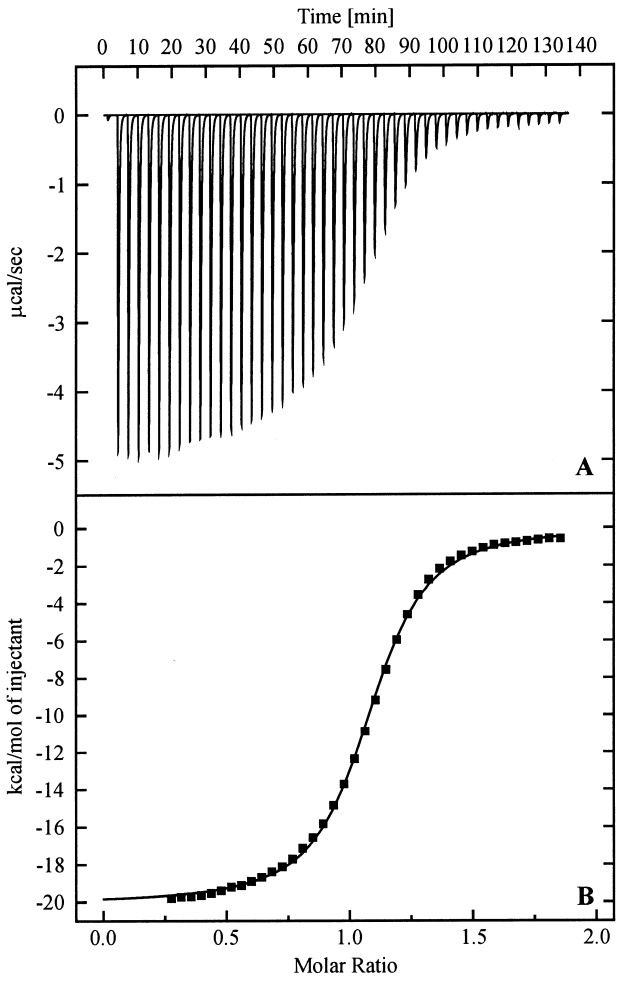

Fig. 1. ITC profile of $^{1}F1^{2}F1$ with B3. A: Heat differences obtained from 45 injections. B: Integrated curve with experimental points (■) and the best fit (–). Data were fitted using a one-site model resulting in: stoichiometry $N = 1.081 \pm 0.002$; $K_D = 1.53 \pm 0.05$ μM; $\Delta H = -20\,070 \pm 60$ cal mol^{-1}; $\Delta S = -40.68$ cal mol^{-1} K^{-1}.

3. Results and discussion

3.1. $^{1}F1^{2}F1$ and B3 form a 1:1 complex in solution

ITC is now a widely applied method for characterization of the thermodynamic parameters of molecular interactions in solutions [24]. Experimental data were fitted with a non-linear function describing an interaction with one binding site. The stoichiometry of the $^{1}F1^{2}F1$/B3 complex was 1:1 within the margins of error in protein concentration measurement and the dissociation constant was 1.5 μM. This is in good agreement with data acquired previously using fluorescence polarization (2.9 μM) [8]. Fig. 1 shows data of a typical ITC experiment. The interaction appears to be exothermic with an unfavorable entropy.

3.2. Mapping the B3 binding site on $^{1}F1^{2}F1$

Fig. 2A shows an overlay of HSQC spectra of uniformly labeled ^{15}N-labeled $^{1}F1^{2}F1$ with and without B3. The addition of B3 causes significant backbone amide chemical shift changes for many $^{1}F1^{2}F1$ residues. The HSQC spectrum of the complex was assigned using 3D NOESY and TOCSY experiments. These experiments were also used to measure changes in H^{α} chemical shifts. It appears that the overall secondary structure of the modules is similar in the complex to that determined for $^{1}F1^{2}F1$, with a similar pattern of interstrand nuclear Overhauser effects observed (data not shown). The changes in backbone chemical shift on binding to B3 are summarized in Fig. 3.

Chemical shift changes of similar magnitude are observed in both modules, suggesting that both modules are involved in binding to B3. The solution structure of the N-terminal module pair $^{1}F1^{2}F1$ of human fibronectin has been resolved recently [10]. In marked contrast to $^{4}F1^{5}F1$, the two modules are separated by a relatively long intermodule sequence and do not form any interface. Hence, the relative orientation of the modules with respect to each other is not well defined. In Fig. 2B, the changes in $^{1}F1^{2}F1$ H^{α} chemical shift on binding to B3 are mapped onto the lowest energy structure of unbound $^{1}F1^{2}F1$ [10].

In both $^{1}F1$ and $^{2}F1$, residues that undergo the largest changes in chemical shifts are in strand E and the D–E loop. In addition, large chemical shift changes were observed in strand A. Although the residues in strand A and E are well separated in the F1 sequence, they are in relatively close proximity in the F1 fold. In binding of D3 to $^{4}F1^{5}F1$, the largest

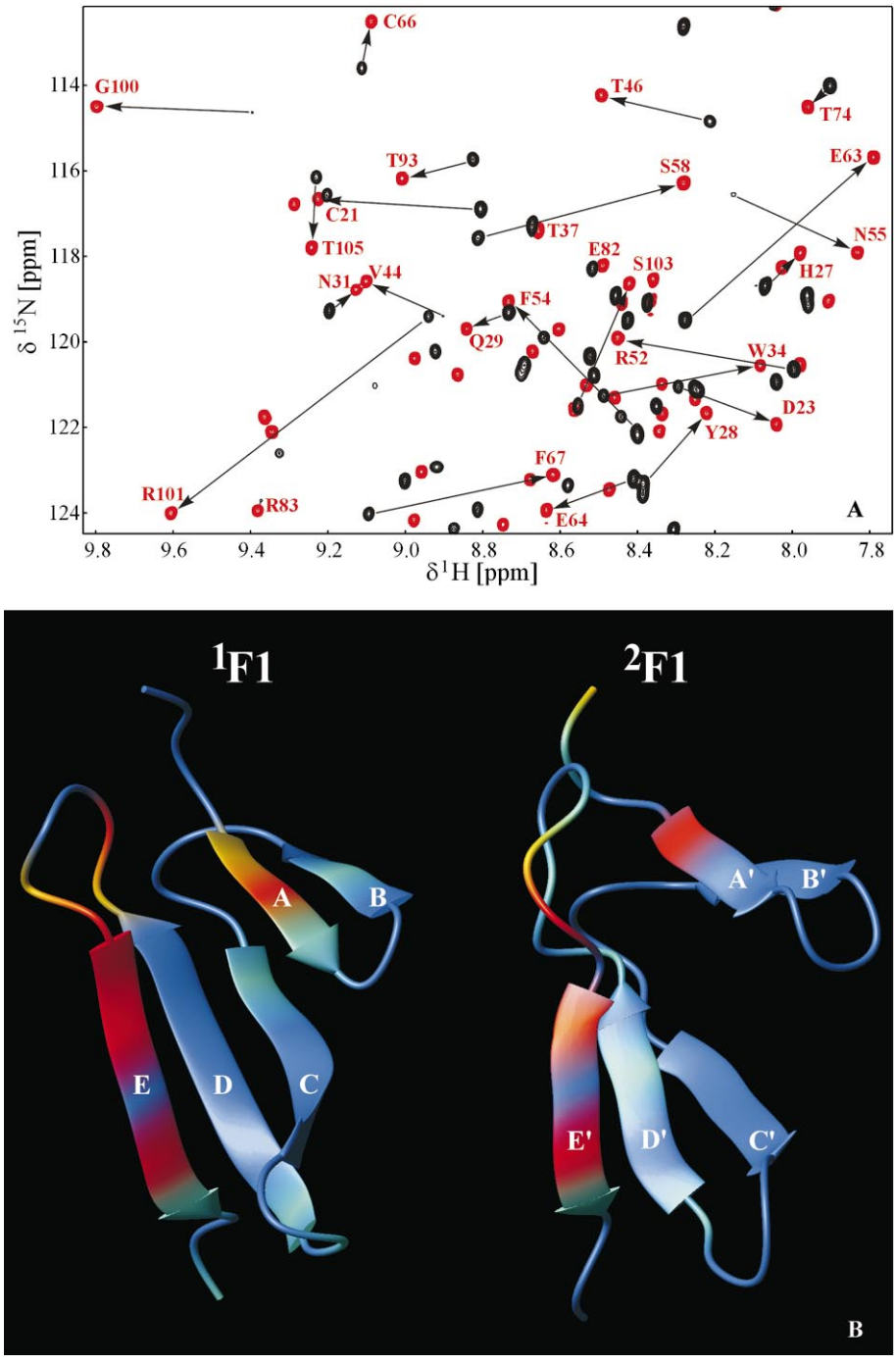

Fig. 2. A: Overlay of a region of ^{1}H, ^{15}N HSQC spectra of 0.25 mM [^{15}N]$^{1}F1^{2}F1$ without (black) and in presence of 0.5 mM B3 (red), recorded at 600 MHz, 25°C, pH 5.0. The arrows indicate the direction of the chemical shift changes on addition of B3. B: Ribbon diagram of uncomplexed $^{1}F1^{2}F1$ with B3-induced H^{α} chemical shift changes (see Fig. 3C). The modules are drawn separately as the relative orientation of the two modules is poorly defined in calculated structures of the module pair [10]. Residues with chemical shift changes ≥ 0.4 ppm, ≥ 0.3 ppm, ≥ 0.2 ppm and ≥ 0.1 ppm are shown in red, orange, yellow and turquoise, respectively. All other residues are shown in blue. The diagram was prepared using MOLMOL [25]. β-Strands of $^{1}F1^{2}F1$ are labeled.

chemical shift changes were also observed for residues in the D–E loop and E strand of $^{4}F1$ [7]. Thus, although they bind to different F1 module pairs, the *S. aureus* and *S. dysgalactiae* FnBPs appear to utilize a similar surface of the F1 module.

4. Concluding remarks

Using a differential labeling approach to distinguish signals of two protein species, we were able to detect the residues in $^{1}F1^{2}F1$ which are involved in binding to B3, a peptide derived from a surface FnBP of the pathogen *S. dysgalactiae*. According to chemical shift changes, both modules of $^{1}F1^{2}F1$ are involved in the interaction. The bacterial peptide appears to utilize a similar surface of the F1 module as an *S. aureus* FnBP in its interaction with the $^{4}F1^{5}F1$ module pair.

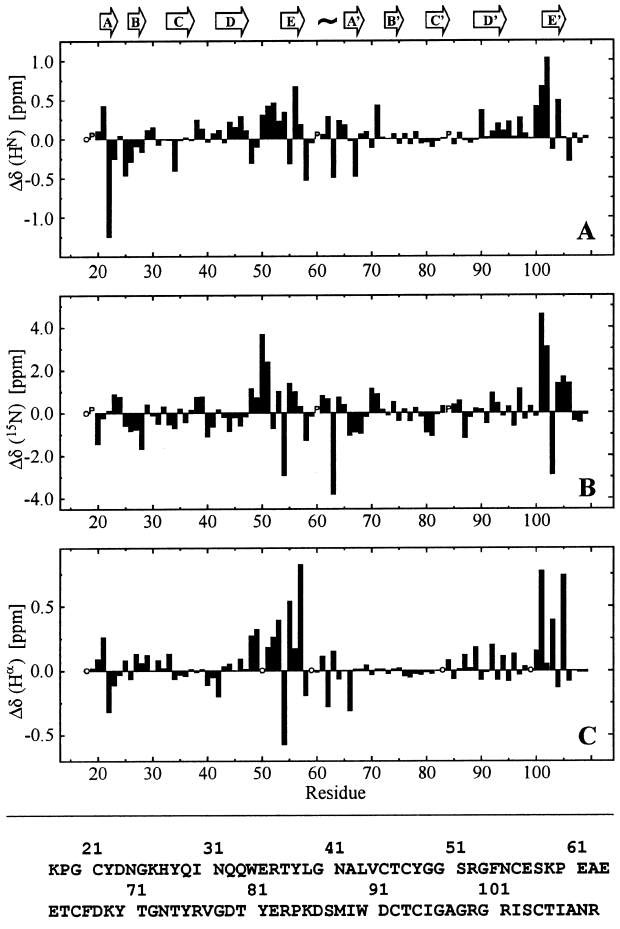

Fig. 3. Backbone chemical shift changes of $^{1}F1^{2}F1$ on binding of B3 at 25°C, pH 5.0 ($\Delta\delta = \delta_{bound} - \delta_{free}$). A: Change in backbone amide ^{1}H shift. B: Change in backbone amide ^{15}N shift. C: Change in H^{α} shift. P stands for prolines; open circles indicate residues for which data were not obtained. The $^{1}F1^{2}F1$ secondary structure is shown at the top of the figure where the linker region is indicated by ~. The amino acid sequence of $^{1}F1^{2}F1$ (residues 17–109 of human fibronectin) is shown at the bottom.

Acknowledgements: This research was supported by the Wellcome Trust, the Biotechnology and Biological Sciences Research Council, the Medical Research Council and the Engineering and Physical Sciences Research Council. This is a contribution from the Oxford Centre for Molecular Sciences. U.S.-L. thanks the Deutsche Forschungsgemeinschaft for a fellowship. J.R.P. and A.R.P. would like to thank the Wellcome Trust for financial support. The authors thank Dr. Jörn M. Werner for very helpful discussions and Dr. Robin Aplin for mass spectrometry.

References

[1] Kuusela, P. (1978) Nature 276, 718–720.
[2] Flock, J.-I., Fröman, G., Jönsson, K., Guss, B., Signäs, C., Nilsson, B., Raucci, G., Höök, M., Wadström, T. and Lindberg, M. (1987) EMBO J. 6, 2351–2357.
[3] Patti, J.M., Allen, B.L., McGavin, M.J. and Höök, M. (1994) Annu. Rev. Microbiol. 48, 585–617.
[4] Hienz, S.A., Schennings, T., Heimdahl, A. and Flock, J.I. (1996) J. Infect. Dis. 174, 83–88.
[5] Peacock, S.J., Foster, T.J., Cameron, B.J. and Berendt, A.R. (1999) Microbiology 145, 3477–3486.
[6] Potts, J.R. and Campbell, I.D. (1994) Curr. Opin. Cell Biol. 6, 648–655.
[7] Penkett, C.J., Dobson, C.M., Smith, L.J., Bright, J.R., Pickford, A.R., Campbell, I.D. and Potts, J.R. (2000) Biochemistry 39, 2887–2893.
[8] Joh, D., Speziale, P., Gurusiddappa, S., Manor, J. and Höök, M. (1998) Eur. J. Biochem. 258, 897–905.
[9] McGavin, M.J., Gurusiddappa, S., Lindgren, P.-E., Lindberg, M., Raucci, G. and Höök, M. (1993) J. Biol. Chem. 268, 23946–23953.
[10] Potts, J.R., Bright, J.R., Bolton, D., Pickford, A.R. and Campbell, I.D. (1999) Biochemistry 38, 8304–8312.
[11] Pickford, A.R., Potts, J.R., Bright, J.R., Phan, I. and Campbell, I.D. (1997) Structure 5, 359–370.
[12] Soffe, N., Boyd, J. and Leonard, M. (1995) J. Magn. Reson. Ser. A 116, 117–121.
[13] Hwang, T.-L. and Shaka, A.J. (1995) J. Magn. Reson. Ser. A 112, 275–279.
[14] Shaka, A.J., Keeler, J., Frenkiel, T. and Freeman, R. (1983) J. Magn. Reson. 52, 335–338.
[15] Marion, D., Driscoll, P.C., Kay, L.E., Wingfield, P.T., Bax, A., Gronenborn, A.M. and Clore, G.M. (1989) Biochemistry 28, 6150–6156.
[16] Marion, D., Kay, L.E., Sparks, S.W., Torchia, D.A. and Bax, A. (1989) J. Am. Chem. Soc. 111, 1515–1517.
[17] Kay, L.E., Keifer, P. and Saarinen, T. (1992) J. Am. Chem. Soc. 114, 10663–10665.
[18] Bodenhausen, G. and Ruben, D.J. (1980) Chem. Phys. Lett. 69, 185–189.
[19] Jeener, J., Meier, B.H., Bachmann, P. and Ernst, R.R. (1979) J. Chem. Phys. 71, 4546–4553.
[20] Kumar, A., Ernst, R.R. and Wüthrich, K. (1980) Biochem. Biophys. Res. Commun. 95, 1–6.
[21] Macura, S. and Ernst, R.R. (1980) Mol. Phys. 41, 95–117.
[22] Braunschweiler, L. and Ernst, R.R. (1983) J. Magn. Reson. 53, 521–528.
[23] Davis, D.G. and Bax, A. (1985) J. Am. Chem. Soc. 107, 2820–2821.
[24] Doyle, M.L. (1997) Curr. Opin. Biotechnol. 8, 31–35.
[25] Koradi, R., Billeter, M. and Wüthrich, K. (1996) J. Mol. Graph. 14, 29–32, 51–55.